

Multi-component kinetic–spectrophotometric analysis. Selection of wavelength and time ranges

Hortensia Iturriaga, Jordi Coello, Santiago MasPOCH* and Marta Porcel

Departament de Química, Facultat de Ciències, Universitat Autònoma de Barcelona, Unitat de Química Analítica, Edifici Cn, E-08193 Barcelona, Spain

Received 6th February 2001, Accepted 14th May 2001

First published as an Advance Article on the web 21st June 2001

An empirical method for the selection of the best wavelength and time ranges which can be used in the quantification of binary mixtures, in a kinetic–spectrophotometric system, is proposed. It is based on finding those ranges which provide the least correlation between the kinetic profiles and the spectra of the products of reaction. The method was applied to the analysis of binary mixtures using simulated data with different rate constant ratios and in the presence of an interference that shows spectral overlap with the analytes. Subsequently, the proposed method was applied to the resolution of dyphylline and proxiphylline mixtures. The system studied was characterized by an elevated similarity in the kinetic behavior of the analytes under pseudo-first-order conditions and an elevated degree of spectral overlap of the products of reaction. In spite of this, satisfactory results were obtained in the quantification of the two analytes. The standard error of prediction (SEP) and the standard deviation between replicates (SDBR) did not show significant differences, being of the order of 4 and of 3% for dyphylline and proxiphylline, respectively.

Introduction

Since the appearance of diode array spectrophotometers, which allow the complete registry of a UV–Vis spectrum in tenths of a second, and of multivariate calibration methods,¹ spectrophotometric resolution of mixtures has been converted into a routine analytical tool. The application of this methodology to kinetic–differential analysis² has considerably widened its analytical possibilities since the resolution can be performed on the basis of a spectral discrimination and also on basis of the different reaction rates, both aspects having a synergetic effect.

The application of conventional multivariate calibration techniques [*e.g.*, partial least squares (PLS)³] to spectral kinetic systems requires the unfolding of the intrinsically three-dimensional matrix (sample, wavelength, time) of the registered data in such a way that the scans recorded at various times are sequentially linked together to form a single row in the *X* data matrix, generating vectors ($\lambda_1 t_1, \lambda_2 t_1, \dots, \lambda_p t_1, \dots, \lambda_1 t_j, \dots, \lambda_1 t_k, \dots, \lambda_2 t_k, \dots, \lambda_p t_k$) of great length (easily of the order of 10 000 terms). It is evident that a great part of this information is very correlated and is redundant and that, in contrast, a certain number of variables cannot contain any type of useful information, which makes a previous selection of the variables advisable. By doing this, the precision of the results is improved.

In early work on wavelength selection in spectroscopic methods, Frans and Harris⁴ demonstrated that the best precision could be obtained with a small number of variables, although that could lead to the loss of other interesting advantages of multivariate calibration.^{1,3} Diverse variable-selection systems have been described, amongst which genetic algorithms^{5–9} stand out owing to their great capacity. Nevertheless, the complexity of calculation and the need to have specific software available make their application difficult. On the other hand, the analyst generally has important previous information available in the resolution of mixtures using spectroscopic data, such as

the spectrum of the products, for which, *a priori*, the spectral zones of maximum sensitivity for each analyte are already known. All of this means that, in practice, rather than searching for an optimal group of discrete variables, spectral modes and wavelength intervals are empirically selected.

This empirical methodology has been extended to kinetic–spectral systems, where both wavelength and time ranges are chosen which are most adequate for the resolution of each mixture. The double information, kinetic and spectral, makes this selection complex, for which the development of simple procedures is advisable. Recently, the index of discrimination¹⁰ has been proposed as a simple means of quantifying the kinetic–spectral discriminating effect of a multi-component system. It is evident that the smaller the coefficients of spectral and kinetic correlation between pairs of analytes, the greater is the difference between their signals and the easier their discrimination will be.

In this work, a simple method for the kinetic–spectral resolution of mixtures on the basis of the selection of the wavelength and time ranges that make their respective coefficients of correlation minimal is proposed. A set of simulated data for the kinetic reaction of two analytes giving two products and one interference with an overlapped spectra was generated in order to check the performance of the proposed method. Several rate constant ratios, producing different kinetic correlations, and several wavelength ranges for different degrees of overlap (interference–analytes) showing different spectral correlations were used. This method was applied to kinetic–spectrophotometric data obtained in the reaction of azo coupling of dyphylline and proxiphylline with the diazonium ion of sulfanilic acid, after alkaline hydrolysis (Fig. 1). Both dyphylline and proxiphylline are substances of pharmacological interest with bronchodilatory properties and have very similar structures, which suggests that their reaction rates and spectra will be very similar.

The chosen reaction was used for the determination of methylxanthines in medicines and has been described in the

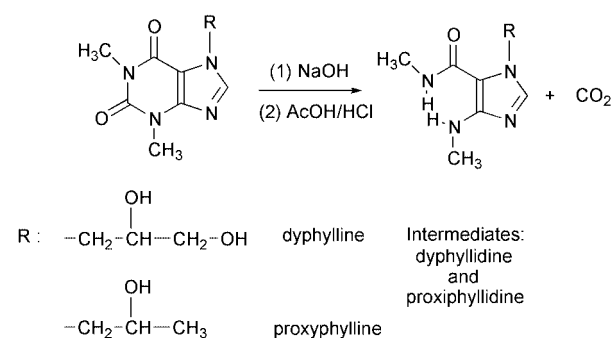
literature,^{11–18} but in no case has it been used for the simultaneous kinetic–spectral resolution of dyphylline and proxyphylline.

Experimental

Simulations

Kinetic–spectrophotometric data for two analytes and a product that interferes in the determination were simulated using a program written using MATLAB v. 5.3 (The Math Works, Natick, MA, USA). The algorithm generates kinetic spectra by solving differential equations and assuming that only the reaction products absorb with Gaussian spectral bands. All the Gaussian bands were constructed with the same width ($\sigma = 60$ nm) and the same absorptivity coefficients every 1 nm over a wavelength range of 100 nm. The maximum of the band for the products of the analytes was kept constant at 23 and 27 nm, and the maximum for the interference was changed to be 40, 50, 60 and 70 nm. In all cases, adherence to Beer's law was presumed for each component and the total absorbance at each wavelength was assumed to be the sum of the absorbances of the components. The analyte concentrations were varied between 1.5×10^{-5} and 5.5×10^{-5} mol dm⁻³ and the interference concentration was kept constant at 1×10^{-5} mol dm⁻³. Data were generated for nine standard calibration mixtures and for 12 unknown mixtures. In order to ensure pseudo-first-order kinetics in relation to the reagent, its concentration was 2.0×10^{-3} mol dm⁻³. Under these conditions, 100 times were used in calculations, simulating that the observed fraction, as reaction, of the slower reacting species (interference) at the end of data collection was 99%. In order to study only the effect of spectral overlap and rate constant variations, the instrumental and rate constant noise contributions were kept constant at 1 and 5%, respectively. These values are based on previously published work.¹⁹

(a) Hydrolysis of the molecules.



(b) Reaction of azo-coupling.

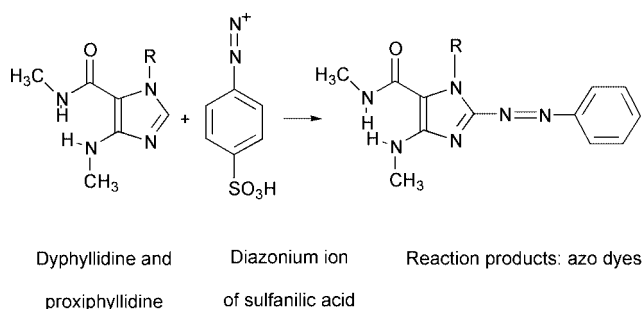


Fig. 1 Reactions of dyphylline and proxyphylline to form the azo coupling products.

A case without interference and four different relative positions of the interference and analytes, generating different spectral overlaps, were studied (Fig. 2). For each situation, four different wavelength ranges were used in the quantification: full spectrum and 30, 50 and 70 points. Finally, three rate constant ratios for the analytes (4, 2 and 1.2) were also considered. The total number of simulations was 60.

Apparatus

A Hewlett-Packard diode array spectrophotometer was used to acquire UV–Vis spectra at 2 nm intervals over the wavelength range 340–540 nm. Scans were performed at 1 s intervals (integration time 0.1 s) for 60 s using a thermostated cell of 1 cm pathlength at 25.0 ± 0.1 °C.

Reagents

All solutions were prepared in water obtained from a Milli-Q water purification system (Millipore). Stock standard solutions containing 7.56×10^{-2} mol dm⁻³ dyphylline [7-(2,3-dihydroxypropyl)theophylline] and proxyphylline [7-(2-hydroxypropyl)theophylline] (from Sigma) were prepared. Volumes of these solutions were mixed and diluted to 5 ml to obtain the working standard solutions.

Citric acid–NaOH buffer (pH 2.65) was prepared with a 0.5 mol dm⁻³ concentration with 1×10^{-3} mol dm⁻³ EDTA from stock standard solutions of citric acid monohydrate (Sigma, ACS reagent), NaOH (Carlo Erba, sodium hydroxide anhydrous pellets, ACS–ISO–f.a.) and EDTA (Panreac, ACS reagent f.a.). A 40% solution of NaOH was prepared as hydrolysis reagent.

A 3.6×10^{-2} mol dm⁻³ stock standard solution of diazonium ion of sulfanilic acid was prepared by mixing an appropriate amount of sulfanilic acid (Fluka, puriss. f.a.; $\geq 99.0\%$) with 1 cm³ of concentrated HCl, 8 cm³ of water and 4 cm³ of 2% NaNO₂ (Aldrich ReagentPlus sodium nitrite, 99.99%). After cooling in an ice-bath for 15 min, 4 cm³ of 2% sulfamic acid (PANREAC f.a.) were added to eliminate the excess of nitrite. Finally, the volume was completed to 25 ml with water.

Procedure

The working standard solutions of analytes were mixed with 5 cm³ of 40% NaOH solution and heated for 1 h at 90 °C, then cooled to room temperature, neutralized with HCl–acetic acid to keep the pH between 5.5 and 6 and diluted to 100 cm³ to obtain the final mixture. Volumes of 2.5 cm³ of buffer, 0.1 cm³ of final mixtures and 0.15 cm³ of diazonium ion of sulfanilic acid were placed, with the aid of micropipettes, directly in the measuring cell. The system was kept at constant temperature with stirring throughout the reaction. The analyte concentrations in the measuring cell were in the range $(1.5\text{--}5.5) \times 10^{-5}$ mol dm⁻³ and were chosen based on the linear ranges obtained with single-analyte experiments. The calibration matrix was constructed following a 3² design and the predictive capacity of the different models tested was assessed by using a prediction set of 12 mixtures containing analyte concentrations within the calibration range. In order to include experimental variability factors, mixtures were prepared and measured in duplicate on different days.

Data processing

The UV–Vis spectra for each sample were recorded at p different wavelengths at k different times in order to construct three-way data arrays which were unfolded to obtain a classical two-dimensional data matrix in such a way that each row contained the spectrum for a mixture recorded at different times sequentially linked together $(\lambda_1 t_1, \lambda_2 t_1, \dots, \lambda_p t_1, \dots, \lambda_1 t_k, \dots, \lambda_2 t_k, \dots, \lambda_p t_k)$, so each column contained the absorbance measured at (λ_i, t_j) for each sample. In order to achieve the best

predictive capacity, different spectral modes (absorbance and first derivative) and working wavelength ranges were tried. The derivative of the data matrix with respect to the wavelength at each time was obtained by using the Savitzky–Golay algorithm with a second-order polynomial and a window size of 11 points.

The data matrix thus obtained was centered and processed by using the PLS1 algorithm in the software Unscrambler v. 7.5 (CAMO, Trondheim, Norway). PLS1 models were constructed by cross-validation method and as many cross-validation segments as samples, each segment comprising the replicates of each sample. The optimum number of PLS1 components was determined in order to minimize the sum of the squared differences between known and determined concentrations:

$$\text{PRESS} = \sum_{i=1}^n (\hat{c}_i - c_i)^2 \quad (1)$$

where n is the number of samples, C_i is the known concentration and \hat{C}_i is the determined concentration.

Two parameters were used to study the precision of the models: the standard error of prediction, SEP, and the standard deviation between replicates, SDBR. The SDBR parameter is calculated starting from the difference between the values obtained for replicates of the same composition, hence it is a measure of the experimental reproducibility, whereas SEP is calculated starting from the differences between the values found and those of reference, taking into account the bias of the values:

$$\text{SEP} = \sqrt{\frac{\sum_{i=1}^n (\hat{c}_i - c_i - \text{Bias})^2}{n-1}} \quad (2)$$

where the symbols have the same meaning as above, and the bias is:

$$\text{Bias} = \frac{\sum_{i=1}^n (\hat{c} - c_i)}{n} \quad (3)$$

The SDBR is defined by the expression:

$$\text{SDBR} = \sqrt{\frac{\sum_{i=1}^k (\hat{c}_{i,1} - c_{i,2})^2}{2k}} \quad (4)$$

where $C_{i,1}$ and $C_{i,2}$ are the determined concentrations of the replicates of each i th sample k is the number of different samples and the other symbols have the same meaning as above.

In the absence of any systematic effect, that is, when the model of calibration adjusts all of the samples well, SEP and SDBR should have similar values, which would indicate that the model of calibration is correct and that the differences found are due solely to experimental reproducibility. To test whether SEP does not vary significantly from the error between replicates, an F test ($\alpha = 0.05$) of significance of the corresponding variances was applied, F being calculated as:

$$F_{\text{calc}} = \frac{\text{SEP}^2}{\text{SDBR}^2} \quad (5)$$

where n is the degrees of freedom from the numerator and k those from the denominator.

Results and discussion

Simulations

One way of assessing the kinetic–spectrophotometric differences between two analytes is through the spectral and kinetic correlations,^{10,20} which are defined mathematically as

$$\rho = \frac{\sigma_{12}}{\sigma_1 \sigma_2} \quad (6)$$

where σ_1 and σ_2 are the standard deviations of the spectral or kinetic profile for analytes 1 and 2 and σ_{12} is the spectral or kinetic covariance between the two.

For the calculation of the kinetic correlation coefficient, ρ_k , the variation of the signal with the time at the maximum of the band (absorbance or derivative) of each of the analytes is used,

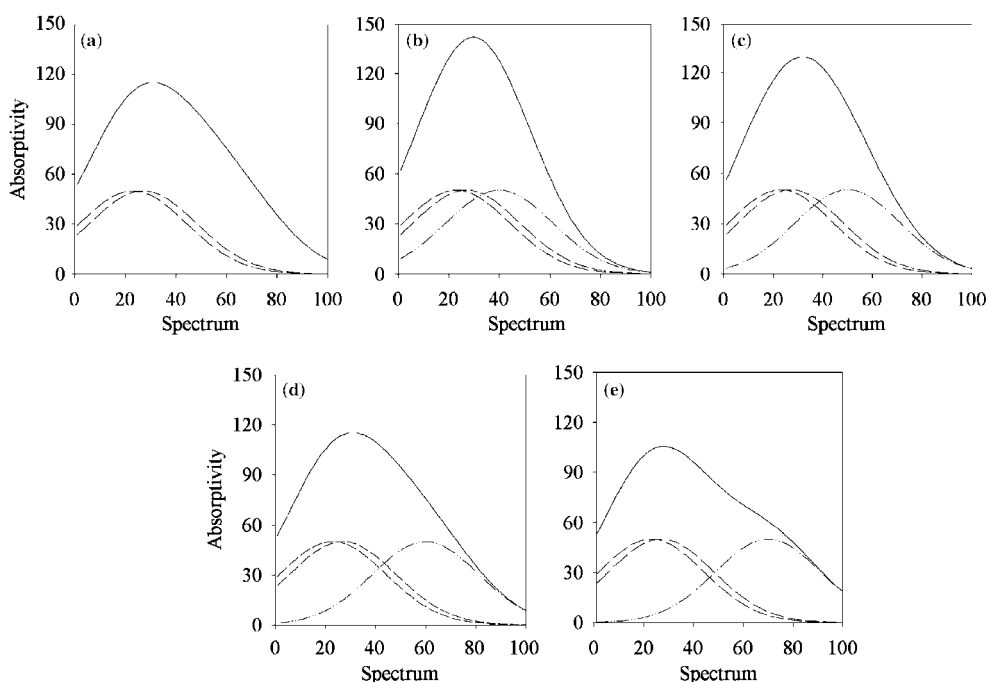


Fig. 2 Spectra of the three absorbing compounds used in the simulations. (---) Reaction products of the analytes; (- · - ·) interference; (—) overall spectrum. (a) Without interference. Maximum of the interference at (b) 40, (c) 50, (d) 60 and (e) 70 nm.

whereas for the calculation of the spectral correlation coefficient, ρ_s , the spectrum of the reaction products of each of the analytes is used, in the mode considered (absorbance or derivative). A correlation coefficient close to unity means that the two analytes behave very similarly, so poor resolution is to be expected. On the other hand, a correlation coefficient close to zero reflects a great kinetic or spectral difference between analytes and the fact that the mixtures can be accurately resolved.

Fig. 3(a) shows the trend of ρ_k with the reaction time for the three rate constant ratios studied. As expected, the more similar the rate constants were, the higher were the kinetic correlations. A constant value of ρ_k is found when the reaction is completed. In Fig. 3(b), the variation of ρ_s with the wavelength range is plotted. Each curve represents a spectral overlap between the interference and the reaction products. As indicated, four different spectral ranges were used for the quantification of the analytes by means of a PLS1 regression.

The results obtained for both analytes in all the simulations as a function of the product $\rho_k \rho_s$ are displayed in Fig. 4. This product could be understood as a simple measure of the overall kinetic-spectrophotometric difference between the two analytes. At low values, it is evident that sufficient information exists to resolve the system correctly, but beyond a certain value, around 0.98, there is not enough spectral and kinetic discrimination and PRESS increases considerably. This threshold should not be taken as an absolute value as it will depend on the noise level of the system studied.

Chemical system

The azo coupling reaction of the methylxanthines has been used previously in quantitative analysis using different coupling

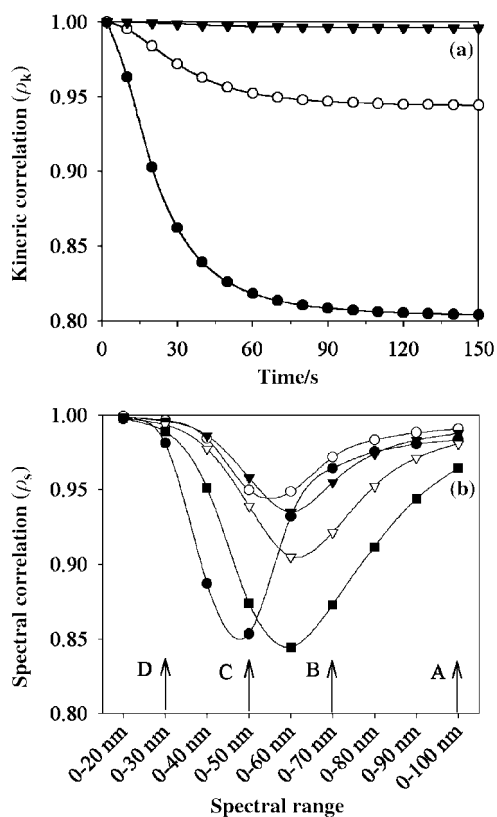


Fig. 3 (a) Variation of the kinetic correlation coefficient with time for different rate constant ratios: (●) $k_1/k_2 = 4$; (○) $k_1/k_2 = 2$; (▼) $k_1/k_2 = 1.2$ (b) Variation of the spectral correlation with the wavelength range; (●) no interference; (○) interference at 40 nm; (▼) interference at 50 nm; (▽) interference at 60 nm; (■) interference at 70 nm. Arrows A, B, C and D indicate the wavelength ranges assayed in the quantification of the analytes.

reagents.¹¹⁻¹⁸ Neither dyphylline nor proxiphylline reacts directly and a previous hydrolysis of the pyrimidine-like ring in an alkaline medium is necessary. Thus, the global process is divided into two stages as can be seen in Fig. 1. This process is influenced by factors such as the concentration of NaOH, the time for hydrolysis, the buffer, the pH, the reagent concentration and the preparation conditions. All of these factors were taken into account when designing the method and in the calibration process.

In the first stage, a study of NaOH concentration and the time of hydrolysis was made, the latter being one of the most determining factors for the analysis of the mixtures. The NaOH/analyte molar ratio was of the order of 500:1 and the optimum hydrolysis time was 60 min.

Prior to the process of azo coupling, neutralization was carried out owing to the elevated concentration of NaOH used in the first stage. This change of pH was accompanied by the release of CO_2 as is described in the literature for species of the same family.^{21,22} The reactions of azo coupling take place very quickly at basic pH, and for this reason an acidic pH was chosen in order to permit spectrophotometric monitoring of the reaction. To carry out the pH study, citric acid-NaOH buffer was chosen. Between pH 2 and 4, the reaction rate of both species did not vary considerably, dyphylline always being the compound which showed a greater apparent reaction rate. pH 2.65 was used for performing the calibration. A concentration of the diazonium ion of sulfanilic acid of $2 \times 10^{-3} \text{ mol dm}^{-3}$ was chosen in the measuring cell with sufficient excess so that the kinetics were of pseudo-first order with respect to the analytes.

Fig. 5 shows the kinetic-spectrophotometric spectra for the reaction of $2 \times 10^{-3} \text{ mol dm}^{-3}$ diazonium ion of sulfanilic acid with a mixture of $3.5 \times 10^{-5} \text{ mol dm}^{-3}$ dyphylline and proxiphylline at pH 2.65 and 25 °C. There is a band between 340 and 390 nm which increases over time and another between 390 and 440 nm which initially increases quickly but after 3 s begins to decrease. Under these experimental conditions, both dyphylline and proxiphylline exhibit a reaction time of about 60 s. As can be seen in Fig. 6, both the absorbance and the derivative spectra for the reaction products are very similar. Thus, both the kinetic and spectral information was necessary to allow the analysis of mixtures.

Determination of dyphylline and proxiphylline mixtures

The correlation coefficients can be used for selecting the range of wavelengths and the total recording time which provide the greatest discrimination between dyphylline and proxiphylline. The first-derivative spectrum was used in this work to carry out

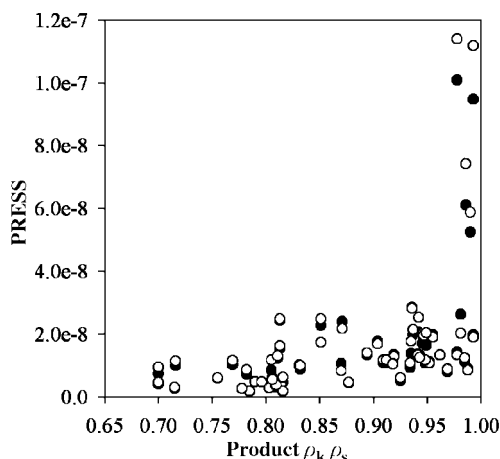


Fig. 4 Variation of PRESS with the product $\rho_k \rho_s$. (●) Fast analyte; (○) slow analyte.

the study of the ranges of wavelengths and time since it corrects the deviation of the baseline and increases the spectral resolution.

From the first-derivative spectrum in Fig. 6(b) for both species, a wavelength of 378 nm was chosen for calculating the kinetic correlation at different time intervals. In Fig. 7(a), it can be seen how the correlation diminishes with increase in recording time up to 60 s, after which point the correlation begins to slightly increase. Hence, this time was chosen as optimum for the recording of the mixtures and for the PLS1 calculations.

A greater difficulty was experienced in the selection of the range of wavelengths since the kinetics of the system showed two apparently important bands for the correct resolution. The starting point was from the derivative spectrum to infinite time [Fig. 6(b)] for each of the analytes, so the kinetic correlation

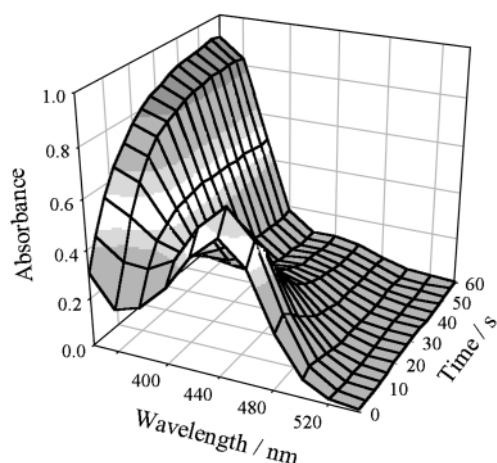


Fig. 5 Kinetic-spectrophotometric spectra for the reaction of a mixture of $3.5 \times 10^{-5} \text{ mol dm}^{-3}$ dyphylline and $3.5 \times 10^{-5} \text{ mol dm}^{-3}$ proxyphylline with $2 \times 10^{-3} \text{ mol dm}^{-3}$ diazonium ion of sulfanilic acid Citric acid-NaOH-EDTA buffer at pH 2.65 and 25 °C. Spectra were recorded from 0 to 60 s at 1 s intervals over the wavelength range 340–540 nm.

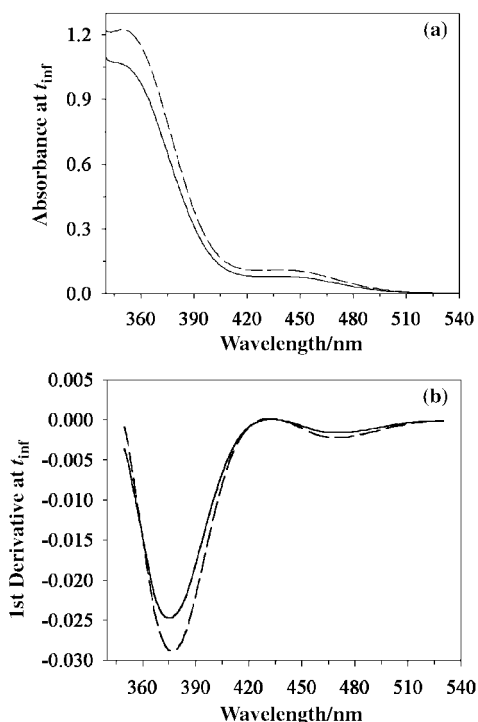


Fig. 6 (a) UV-Vis spectra and (b) first-derivative spectra of the reaction products of dyphylline (—), and proxyphylline (---), both at $1 \times 10^{-4} \text{ mol dm}^{-3}$ concentration with $2 \times 10^{-3} \text{ mol dm}^{-3}$ diazonium ion of sulfanilic acid. Citric acid-NaOH-EDTA buffer at pH 2.65 and 25 °C.

coefficient was fixed and the spectral correlation coefficient for different ranges of wavelengths was calculated. As can be seen, the correlation diminishes as the interval shortens to a minimum, 350–410 nm, from which point it begins to increase again up to almost unity.

SEP and SDBR for the external prediction set are compared in Table 1 for different intervals of wavelengths using a 60 s recording time and it is observed that the best results were obtained in the wavelength interval 350–410 nm, which presented less spectral correlation [Fig. 7(b)] and the minimum value of the product $\rho_k \rho_s$. It is also observed that as the wavelength interval diminishes, the number of variables used in the calculation is reduced, so the models obtained are easier to interpret (Table 1). In cases the results obtained for proxyphylline are better than those for dyphylline, possibly owing to its greater molar absorptivity. A simpler interpretation of the quality of the results can be made by calculating the values of SEP and SDBR relative to the average concentration, these being of the order of 4 and 3% for dyphylline and proxyphylline, respectively. For all of the models, applying the *F* test of significance, the standard errors of prediction in terms of error do not differ significantly from the difference between replicates, hence PLS1 correctly quantifies both analytes. Nevertheless, it is observed that as the selected interval of wavelengths diminishes, the SEP and SDBR values diminish, thus increasing the precision of the models. Table 2 gives the individual results obtained with PLS1 using the wavelength range 350–410 nm for the prediction set. The regression parameters for the prediction of dyphylline are intercept = $(0.46 \pm 1.88) \times 10^{-6} \text{ mol dm}^{-3}$, slope = 0.958 ± 0.051 , $r = 0.992$, and for proxyphylline intercept = $(0.16 \pm 1.75) \times 10^{-6} \text{ mol dm}^{-3}$, slope = 0.981 ± 0.048 , $r = 0.993$.

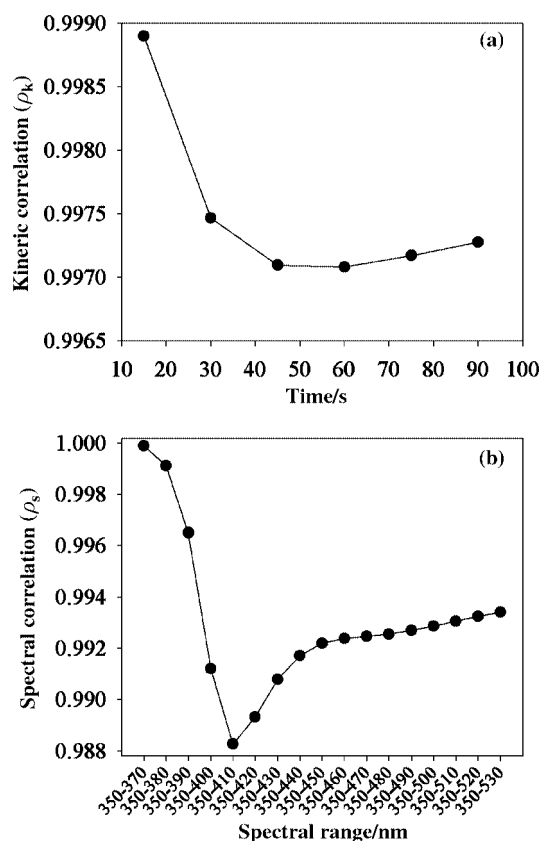


Fig. 7 (a) Variation of the kinetic correlation coefficient (ρ_k) between dyphylline and proxyphylline with the time range. (b) Variation of the spectral correlation coefficient (ρ_s) between the reaction products of dyphylline and proxyphylline with the wavelength range. [Analyte] = $1 \times 10^{-4} \text{ mol dm}^{-3}$; [diazonium ion] = $2 \times 10^{-3} \text{ mol dm}^{-3}$; citric acid-NaOH-EDTA buffer at pH 2.65 and 25 °C.

Table 1 SEP [eqn. (2)] and SDBR [eqn. (4)] obtained in the determination of dyphylline and proxyphylline in the prediction set using PLS1 models and different spectral ranges

Wavelength range/nm	Variable/sample	$\rho_k\rho_s$	Dyphylline ^a		Proxyphylline ^a	
			SEP	SDBR	SEP	SDBR
350–530	5460	0.9910	2.15×10^{-6}	1.86×10^{-6}	1.69×10^{-6}	1.62×10^{-6}
350–470	3660	0.9896	1.95×10^{-6}	1.62×10^{-6}	1.49×10^{-6}	1.38×10^{-6}
350–410	1860	0.9854	1.50×10^{-6}	0.97×10^{-6}	1.18×10^{-6}	0.77×10^{-6}

^a Number of PLS components used in the models = 3.**Table 2** Results obtained in the resolution of mixtures of dyphylline and proxyphylline in the prediction set using PLS1 and the wavelength range 350–410 nm

Sample	Dyphylline ^a			Proxyphylline ^a		
	Added $\times 10^5$ /mol dm ⁻³	Found $\times 10^5$ /mol dm ⁻³	Absolute error $\times 10^5$ /mol dm ⁻³	Added $\times 10^5$ /mol dm ⁻³	Found $\times 10^5$ /mol dm ⁻³	Absolute error $\times 10^5$ /mol dm ⁻³
M1a	2.29	2.23	-0.05	2.28	2.24	-0.04
M1b	2.29	2.21	-0.07	2.28	2.25	-0.03
M1c	2.30	2.27	-0.03	2.30	2.33	0.03
M1d	2.30	2.34	0.04	2.30	2.28	-0.02
M2a	5.29	5.33	0.04	2.28	2.16	-0.12
M2b	5.29	4.98	-0.31	2.28	2.45	0.17
M2c	5.32	5.34	0.02	2.30	2.38	0.08
M3a	3.91	3.95	0.04	2.75	2.68	-0.07
M3b	3.91	4.08	0.17	2.75	2.59	-0.17
M4a	2.97	2.82	-0.15	3.22	3.17	-0.05
M4b	2.97	2.88	-0.09	3.22	3.17	-0.05
M5a	1.85	1.94	0.09	3.44	3.49	0.05
M5b	1.85	1.86	0.01	3.44	3.53	0.09
M6a	4.60	4.51	-0.09	3.44	3.32	-0.12
M6b	4.60	4.47	-0.13	3.44	3.32	-0.12
M7a	3.44	3.28	-0.16	3.66	3.69	0.03
M7b	3.44	3.44	0.00	3.66	3.58	-0.08
M8a	2.29	2.14	-0.15	3.90	3.85	-0.05
M8b	2.29	2.09	-0.20	3.90	3.86	-0.04
M9a	4.85	4.59	-0.26	3.93	3.65	-0.28
M9b	4.85	4.77	-0.08	3.93	3.62	-0.31
M10a	3.66	3.46	-0.20	4.59	4.50	-0.09
M10b	3.66	3.53	-0.13	4.59	4.34	-0.25
M11a	2.75	2.76	0.01	5.03	4.91	-0.12
M11b	2.75	2.62	-0.13	5.03	4.97	-0.06
M12a	4.60	4.11	-0.49	5.28	5.43	0.15
M12b	4.60	4.17	-0.43	5.28	5.33	0.05

^a Number of PLS components used in the models = 3.

Conclusions

A rapid, simple and easily interpreted method for the selection of variables in kinetic–spectrophotometric systems which does not require the use of complicated calculation methods and specific software has been developed. The reduction in the number of variables permits the construction of more rapid models that are easy to interpret, and provides better results since it eliminates the least important information related to the system under study.

Once again it is evident that the PLS1 multivariable calibration technique is a powerful mathematical tool for the kinetic–spectrophotometric resolution of mixtures of analytes which show great spectral overlap and similarity in kinetic behavior as opposed to a common reagent.

Acknowledgements

The authors are grateful to the DGICYT, Spain, for funding this research within the framework of Projects PB97-0213 and PB96-1180. M. Porcel acknowledges additional support from

the Spanish Ministry of Science and Technology in the form of an FPI grant.

References

- 1 H. Martens and T. Naes, *Multivariate Calibration*, Wiley, New York, 1989.
- 2 S. R. Crouch, A. Scheeline and E. S. Kirkor, *Anal. Chem.*, 2000, **72**, 53R.
- 3 T. F. Cullen and S. R. Crouch, *Mikrochim. Acta*, 1997, **126**, 1.
- 4 S. D. Frans and J. M. Harris, *Anal. Chem.*, 1985, **57**, 2680.
- 5 A. S. Barros and D. N. Rutledge, *Chemom. Intell. Lab. Syst.*, 1998, **40**, 65.
- 6 R. Leardi and A. L. González, *Chemom. Intell. Lab. Syst.*, 1998, **41**, 195.
- 7 A. Herrero and M. C. Ortiz, *Anal. Chim. Acta*, 1999, **378**, 245.
- 8 L. G. Weyer and S. D. Brown, *J. NIR*, 1996, **4**, 163.
- 9 M. Azubel, F. M. Fernández, M. B. Tudino and O. E. Troccoli, *Anal. Chim. Acta*, 1999, **398**, 93.
- 10 S. R. Crouch, J. Coello, S. MasPOCH and M. Porcel, *Anal. Chim. Acta*, 2000, **424**, 115.
- 11 P. Depovere, M. Piroux and T. Adzet, *Circ. Farm.*, 1975, **33**, 623.
- 12 J. C. Chiarino, *An. Asoc. Quim. Farm. Urug.*, 1951, **51**, 13.
- 13 H. Raber, *Sci. Pharm.*, 1964, **32**, 122.

- 14 R. Ott and H. Wittmann-Zinke, *Sci. Pharm.*, 1958, **26**, 217.
- 15 M. Mariani-Scotti, *Boll. Chim. Farm.*, 1965, **104**, 356.
- 16 S. R. El-Shabouri, S. A. Hussein and S. E. Emara, *Talanta*, 1989, **36**, 1288.
- 17 G. Fleischer, *Pharmazie*, 1956, **11**, 208.
- 18 M. P. de Castro and R. Rey, *Inf. Quím. Anal.*, 1963, **17**, 158.
- 19 M. Blanco, J. Coello, H. Iturriaga, S. Maspoch, M. Redón and J. F. Rodríguez, *Quím. Anal.*, 1996, **15**, 266
- 20 T. F. Cullen and S. R. Crouch, *Anal. Chim. Acta*, 2000, **407**, 35.
- 21 R. Pohloudek-Fabini, G. Döge and D. Kottke, *Pharmazie*, 1984, **39**, 24.
- 22 G. Peinhardt, *Pharmazie*, 1991, **46**, 812.